JOURNAL OF MATERIALS SCIENCE 27 (1992) 3552–3564

Influence of rapid solidification route on microstructure and properties of a thermally stable Al–Cr–Zr alloy

G. J. MARSHALL
Alcan International Ltd, Banbury Laboratory, Southam Road, Banbury, OX16 7SP, UK
E. K. IOANNIDIS
Department of Materials, Imperial College of Science and Technology, Exhibition Road, London SW7 2BP, UK

An Al–5% Cr–2% Zr (wt%) alloy for elevated temperature service has been rapidly solidified (RS) by gas atomization and planar flow casting (PFC). A comparative study of the atomized powder and the planar flow cast ribbon has been performed during consolidation by extrusion. Particular attention has been given to the microstructural changes during fabrication and the influence of RS particulate type on extrusion performance, microstructure and mechanical properties. Microstructurally it has been shown that the more homogeneous PFC ribbon has advantages over the atomized powder and can improve mechanical properties. However, optimization of the thermomechanical processing of the PFC ribbon is necessary to achieve significant performance benefits in comparison to the atomized powder.

1. Introduction

The thermal stability of Al-rich alloys from the Al–Cr–Zr system has been demonstrated in recent years [1–3]. For service at temperatures up to 350 °C [4, 5], aluminium alloys will need to exploit rapid solidification technologies. This can be achieved by choosing a number of RS routes. The objective of this publication is, firstly, to compare the microstructure, fabrication performance and mechanical properties of an Al–5%Cr–2%Zr (wt%) alloy produced by gas atomization and planar flow casting. Secondly, to correlate the microstructural features of each RS material with their consolidated properties and highlight the essential differences.

Al–Cr–Zr alloys derive their strength and thermal stability from the precipitation of coherent Al_3Zr particles during processing and the retention of some of the Cr in solid solution [1]. The solidification rates during powder atomization successfully supersaturate Zr in solid solution, however, Cr forms dispersoids during solidification and the dispersoid size varies directly with powder particle size. Unfortunately, poor fracture toughness levels have been associated with the presence of these coarse dispersoids in extruded bar [3]. Therefore the use of planar flow casting with its inherently higher solidification rates [6] is being evaluated as a means to eliminate these dispersoids.

2. Experimental procedure

The atomized powder was produced by an inert gas (He/Ar mixture) up-draught technique (supplied by Metalloys, UK) and the planar flow cast ribbon was produced by Allied Corp. USA. The two materials had the following compositions: atomized powder: 5.08% Cr, 2.18% Zr and PFC: 4.99% Cr, 2.26% Zr.

Fabrication of both materials was conducted in two distinct stages: cold compaction and hot extrusion. Cold compaction of ~ 600 g billets was achieved by using a double action piston and tapered die assembly (72 mm diameter) at a pressure of 500 MPa resulting in billet densities of ~ 85%. There was no discernible difference in the compaction behaviour of the two RS materials despite their very different surface to volume ratios. The billets were then rapidly heated, automatically transferred to the preheated container of the extrusion press, extruded and the extrusion bar water-quenched to retain the hot-worked microstructure The complete hot extrusion cycle lasted less than 6 min. Two different extrusion routes were employed, direct and indirect, on the same 5 MN hydraulic press. A narrow temperature range of 425–475 °C was examined to produce 20:1 reduction round bar and 15:1 reduction rectangular bar with an aspect ratio of 4.6:1.

Transmission electron microscopy (TEM) was performed on both transverse and longitudinal sections of selected extrusions. The thin foils were prepared using a conventional jet electropolishing technique with a methanol solution of 5% $HClO_4$ and 1.5% HNO_3 at −40 °C and 40 V. The specimens were examined on a Jeol 2000FX microscope operating at 200 kV. Optical metallography was carried out on samples prepared by standard grinding and polishing

0022–2461

techniques and after etching in Kellers reagent. Fractography was performed on a Jeol T300 scanning electron microscope (SEM).

To aid phase identification in both particulate and consolidated materials, X-ray analysis was conducted using a Philips diffractometer with filtered CuK_{α} radiation.

For assessment of mechanical properties; tensile, Vickers hardness and fracture toughness, specimens were manufactured from selected extruded bars. The fracture toughness was assessed by using the short-rod specimen geometry [7] which has been shown to correlate well with K_{IC} values.

3. Results and discussion

3.1. Rapidly solidified microstructures

The solidification behaviour and solidified microstructure of a range of Al–Cr–Zr alloys from a number of atomizers have been characterized previously [1, 8, 9]. Typical microstructures from the He/Ar atomized powders used in the current investigation were published recently by Palmer *et al.* [3]. The spread of solidification rates experienced by powders of 5–75 μm diameter found in an atomized batch, resulted in an assortment of microstructures. The majority of powder particles contained some Cr-rich dispersoids, identified as $Al_{13}Cr_2$, but only the finest powders ($< 20\,\mu m$) exhibited a uniform distribution of dispersoids. It was predominantly in the coarse powders ($> 50\,\mu m$) that large dispersoids and clusters were observed which were associated with poor fracture properties. The mid-size powders exhibited a mixed microstructure of dispersoids, coarser particle clusters and areas devoid of any precipitation. There were also powders with cellular and partitionless regions which contained no particles. The fine powders with the uniform distribution of dispersoids (~ 50 nm

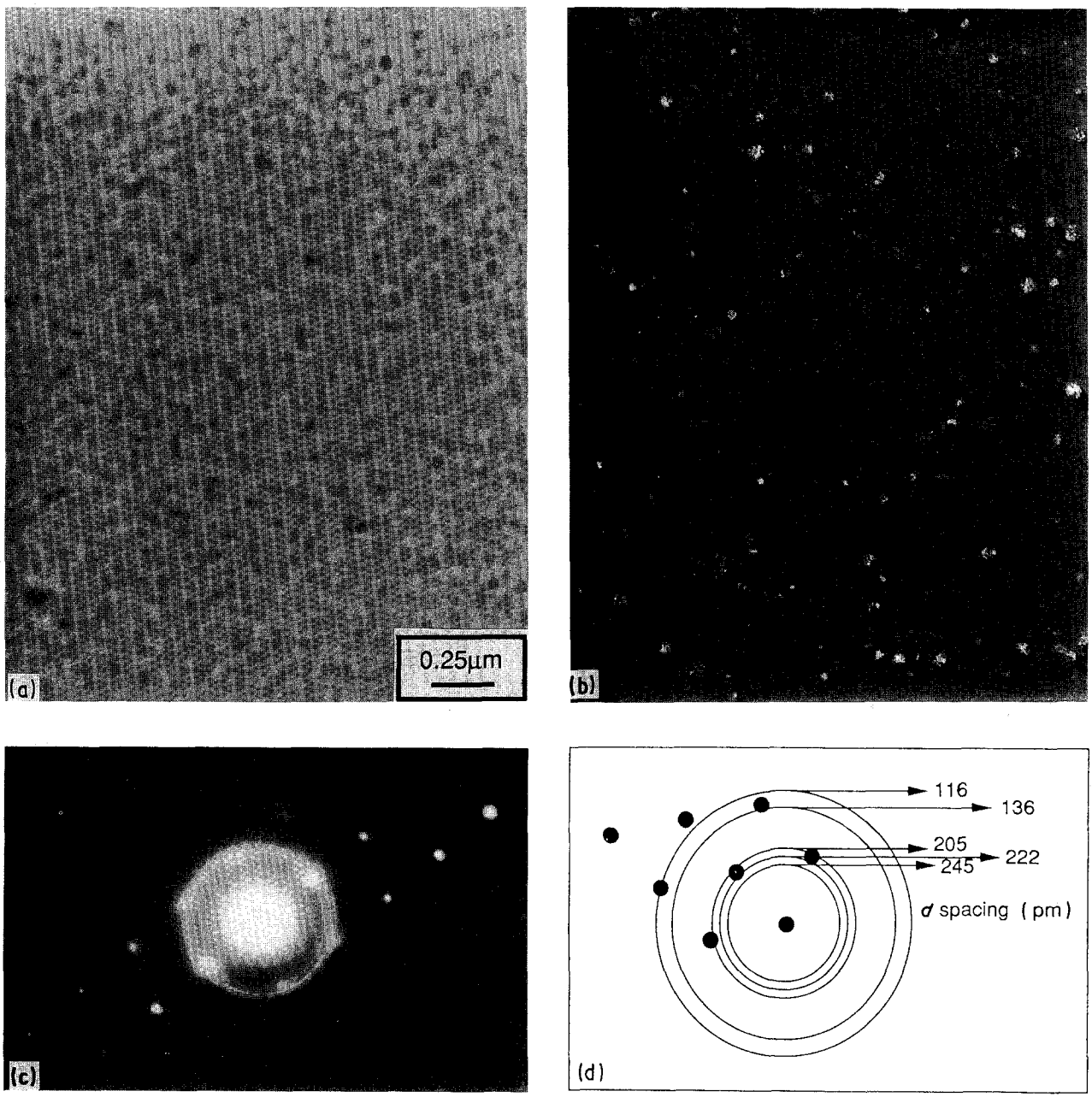

Figure 1 Transmission electron micrograph of the finest powders: (a) bright field; (b) dark field; (c) selected area diffraction pattern and (d) solution.

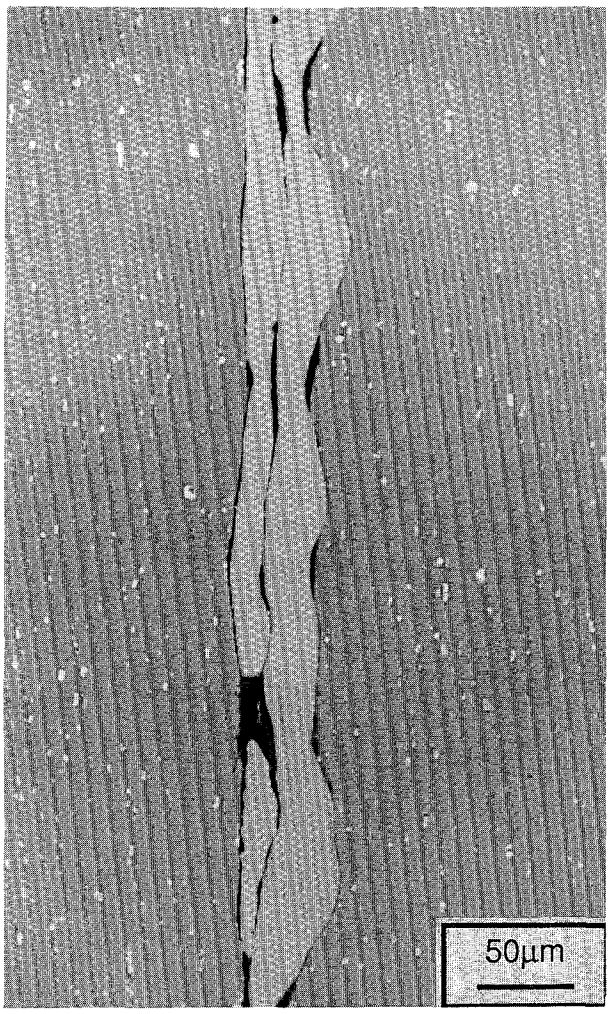

diameter) were found to be extremely stable during subsequent heat treatment [3].

Additional electron diffraction studies of the finest powder revealed that the very fine dispersoids are $Al_{13}Cr_2$, Fig. 1. The ring diffraction pattern indicates that the discrete dispersoids observed have a random orientation with the matrix. Clearly the fact that the equilibrium phase has formed, accounts for the excellent thermal stability of the dispersoids during subsequent heat treatment. An analysis of the solidification behaviour of similar RS alloys carried out by one of the authors [9], suggested that high Cr contents promoted the nucleation of $Al_{13}Cr_2$ in the liquid droplet in peritectic manner. However it is still not clear why partitionless solidification should then occur as particle size increases which has been observed in the present alloy.

A detailed examination of the PFC ribbon was carried out such that the essential features could be compared with the powders. In contrast to the powder, no coarse dispersoids were observed in the PFC when examined by scanning electron microscopy, Fig. 2. The Cr-rich dispersoids would have been easily identified using back-scattered electron imaging which depends upon atomic number contrast. The cross-section shown in Fig. 2 is normal to both the casting direction and the wheel used in planar flow casting

Figure 2 Scanning electron micrograph of PFC as-cast ribbon, sandwiched between Al alloy supports containing coarse particles.

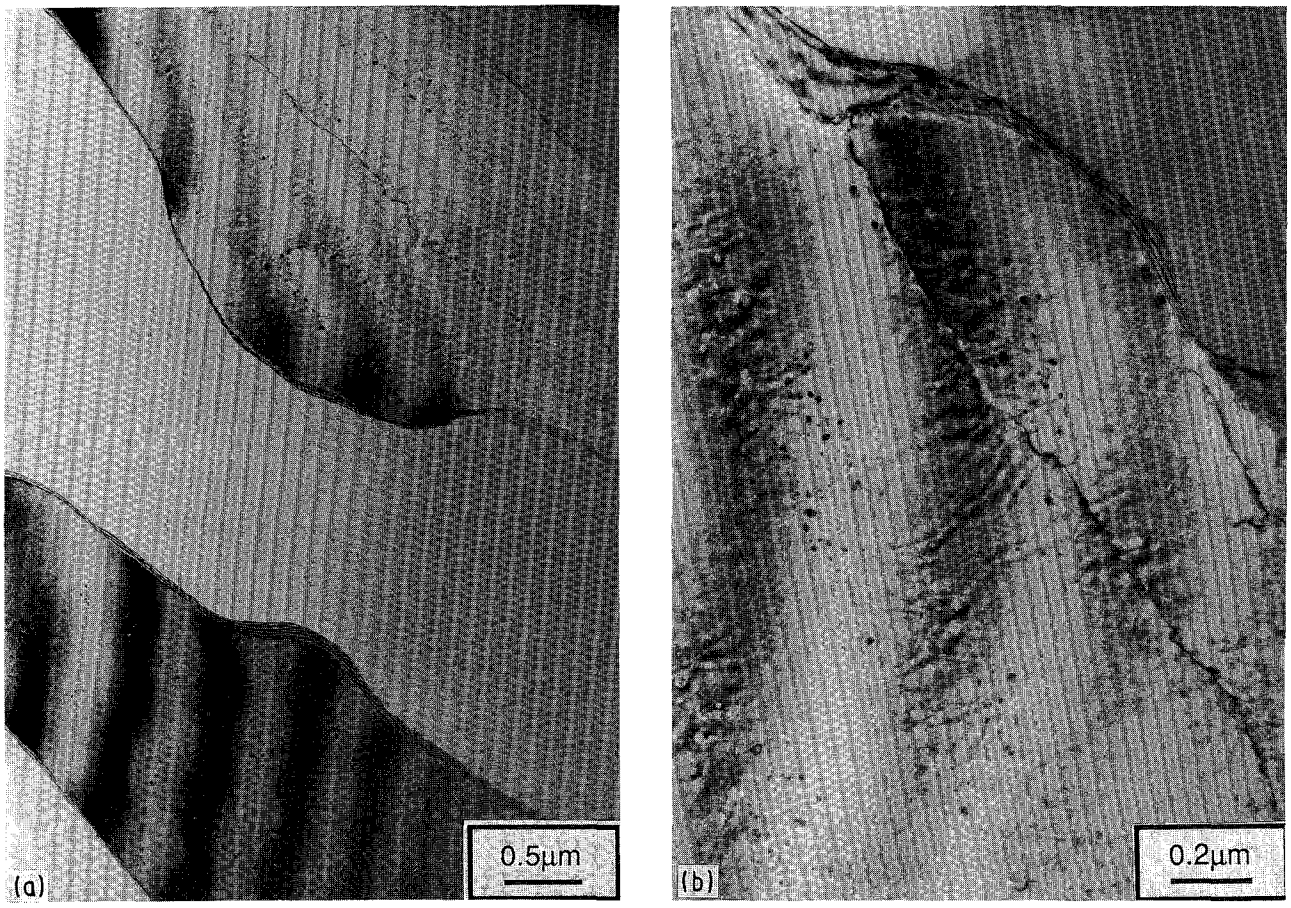

Figure 3 Structure within the thin region of PFC ribbon. Note the cellular morphology (a) and the presence of fine precipitation (b).

TABLE I X-ray data of particulates

Intermetallic compound	Atomized powder			PFC ribbon		
	A.R.	350 °C/24h	500 °C/2h	A.R.	350 °C/2h	450 °C/2h
$Al_{13}Cr_2$	Medium	Medium	Strong	Weak	Medium	Strong
Al_3Zr cubic	Weak	Strong	[a]	Not detected	Weak	Strong
Unidentified	Medium	Medium	[b]	Weak	Medium	Medium

[a] masked by matrix?
[b] not assessed

TABLE II Relative intensities for various *d* spacings

d spacing (pm)	Relative intensities (%)
258	25
245	100
239	25
230	60
229	60
228	40
210	50

and shows a variable thickness of 5–40 μm. The as-solidified structure from the thin regions of the ribbon showed a cellular morphology within an anisotropic grain structure, Fig. 3a. Segregation of Cr and Zr to the cell centres (both elements have a partition coefficient significantly greater than one) has caused fine scale precipitation and the formation of dislocation loops, see Fig. 3b. It has not been possible to positively identify these fine precipitates using electron diffraction or microanalysis (see later). Typical microstructures of the bulk of the ribbon are shown in Fig. 4. Precipitates (< 30 nm) have formed within the grain interior and also at grain boundaries creating a small precipitate free zone. This precipitate morphology indicates that a solid state reaction had occurred during cooling of the solidified ribbon. X-ray data, Table I, for both particulate shows that an unidentified phase (or phases), see Table II, in equal strength to $Al_{13}Cr_2$ is present in both powder and PFC. Thus highlighting the difficulty in determining the nature of the precipitates in the PFC. Recent work by Octor and Naka [10] claims to have identified similar precipitates in Al–Cr–Zr melt-spun ribbon as $Al_{13}Cr_2$. The absence of meta-stable Al_3Zr reflections from the PFC ribbon suggest that the Zr has been supersaturated during solidification. In other regions, presumably experiencing slower solidification or cooling rates, a distribution of dispersoids had formed, Fig. 5a. Although relatively small in size (< 200 nm), their morphology is different to that of the fine dispersoids within the finest of the atomized powders. Again, it appears that these dispersoids have formed during cooling of the solidified ribbon. A further feature of the PFC ribbon was the appearance of a few nodular dispersoids, Fig. 5b, similar to those in the powders but with diameters less than 0.5 μm.

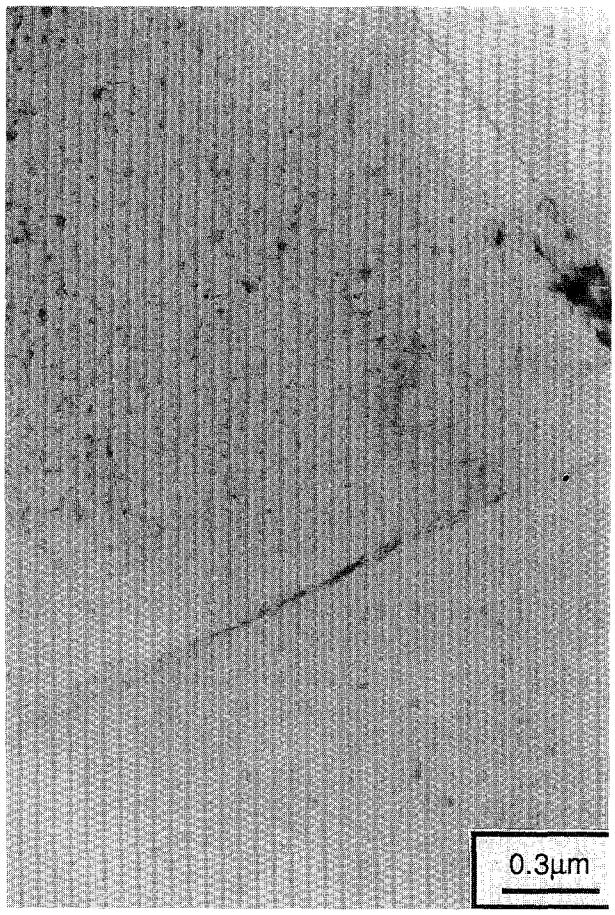

Figure 4 Typical microstructure from the ribbon.

It is evident that the PFC ribbon has a more homogeneous microstructure than encountered in the range of powders from the atomized batch. In particular, the Cr-rich dispersoids are more uniformly distributed and finer, thus eliminating the very coarse particles that were reported as being detrimental to the consolidated powder properties. As a word of caution, it should be noted that the PFC ribbon, unlike the powder, was chopped prior to consolidation and this additional step may influence the subsequent development of microstructure due to the cold work imparted. The stored strain energy may affect the decomposition of the supersaturated matrix during billet preheating which was typically 350–450 °C for extrusion. It is also possible that the higher dislocation density in the chopped PFC may encourage heterogeneous precipitation of equilibrium

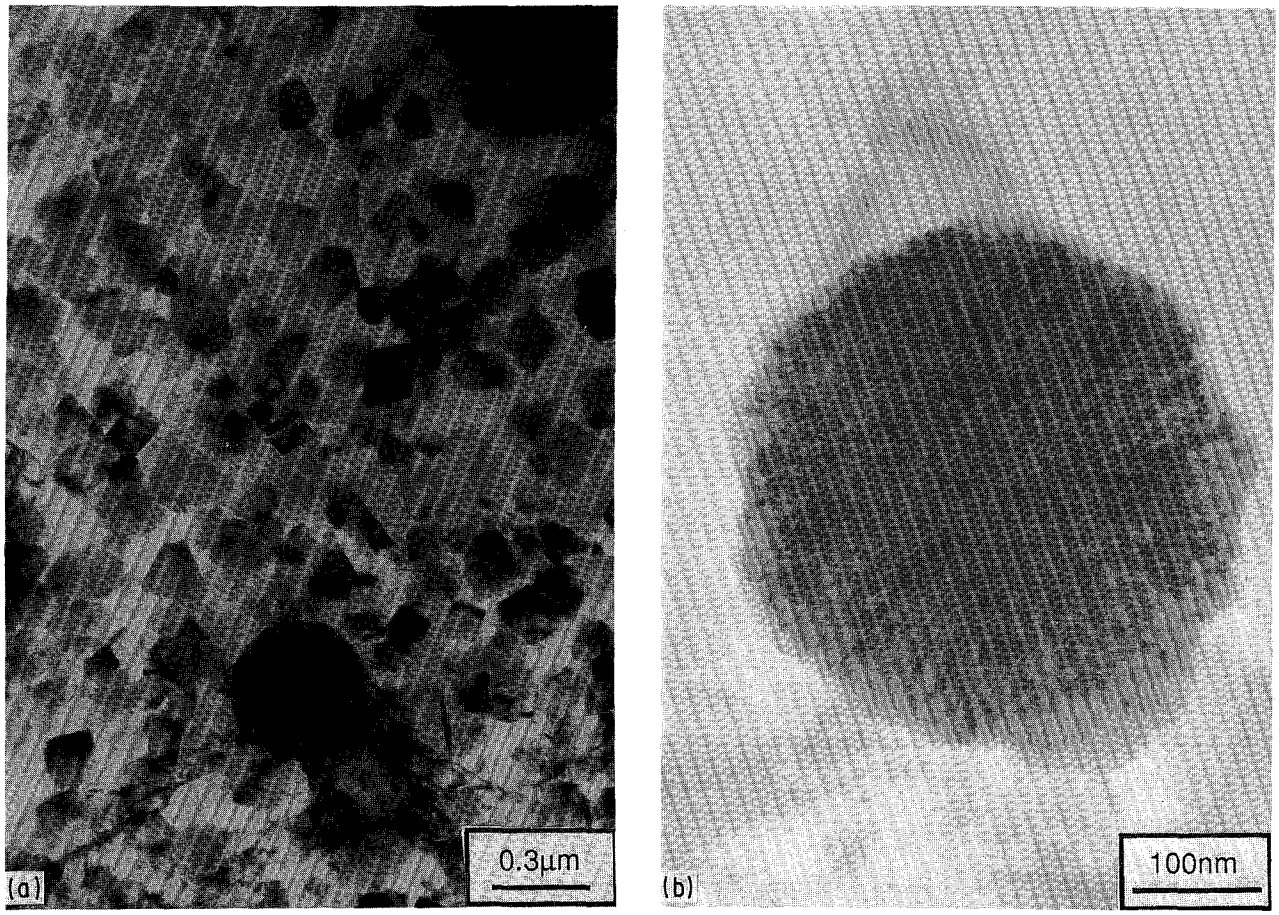

Figure 5 (a) Dispersoids formed in the thicker ribbon regions and (b) occasional nodular particulate.

Al_3Zr in preference to the meta-stable cubic Al_3Zr desired for maximum strengthening.

It has been shown that the presence of surface oxide formed during rapid solidification reduces the properties of the consolidated particulate [11]. Previous work [8] on powders has shown that the oxide thickness is independent of the solidification route and atomizing environment and therefore the PFC ribbon should be equivalent to the powder (no attempt has been made to measure the thickness of the oxide on the PFC ribbon). However, the ribbon which is 30 μm thick on average, will have 25% more surface area than a spherical powder particle of equivalent volume. Hence the increased volume fraction of oxide may off-set the benefits of the homogeneous ribbon microstructure.

3.2. Consolidation

Laboratory scale and semi-commercial extrusion of the atomized powders and to much lesser extent the PFC have been reported previously [3]. To optimize mechanical properties, an extrusion temperature of $< 400\,^{\circ}C$ was determined to prevent overageing of the Al_3Zr precipitates and removal of Cr from solid solution [1]. However this is not always possible with conventional direct extrusion which utilizes reduction ratios of $> 20:1$. One alternative is the use of indirect extrusion which removes billet to container wall friction and therefore reduces the maximum pressure requirement. Hence this allows a lower extrusion temperature normally limited by the high pressure needed to extrude thermally stable aluminium alloys. Therefore an objective of the current study was to examine the potential benefit of indirect extrusion using a laboratory press whilst still comparing the behaviour of both powder and PFC.

The pressure requirements for the laboratory scale extrusion are shown in Fig. 6 for both atomized powder and PFC. Data is given for peak and steady state pressures during direct and indirect extrusion at three temperatures. Firstly the results show the benefit of indirect extrusion which reduced the peak pressure requirement by 10–35% depending on material and temperature. This is significant because the peak pressure requirement determines the minimum extrusion temperature that is possible. In contrast, there was little or no reduction in steady state pressure when changing from direct to indirect extrusion. Secondly, a comparison of the two RS particulate indicated that the powder required lower peak pressures for indirect extrusion and slightly lower steady state pressures for both indirect and direct modes. It appears that during direct extrusion the peak pressure was more dependent on the friction conditions than the difference in the two materials.

There are two possible reasons for the reduced pressure requirements during powder extrusion. The PFC ribbon may simply be stronger, either due to its initial state or to precipitation during preheating to the extrusion temperature. It is expected that the more homogeneous microstructure of the ribbon will be an

effective strengthener upon decomposition due to the supersaturated solid solution and fine dispersoids. Indeed the X-ray data indicates that the PFC ribbon decomposes during heat treatment to form the cubic Al_3Zr phase. A less likely alternative, is strengthening derived from the higher oxide content of the PFC since it is generally observed that the oxide film forms a fine dispersion during consolidation and does strengthen dilute aluminium powder alloys. To examine these possibilities, billets of both particulate were partially extruded and then sectioned for microstructural examination.

Decomposition of the He/Ar atomized powder has been reported previously [3] and showed that the

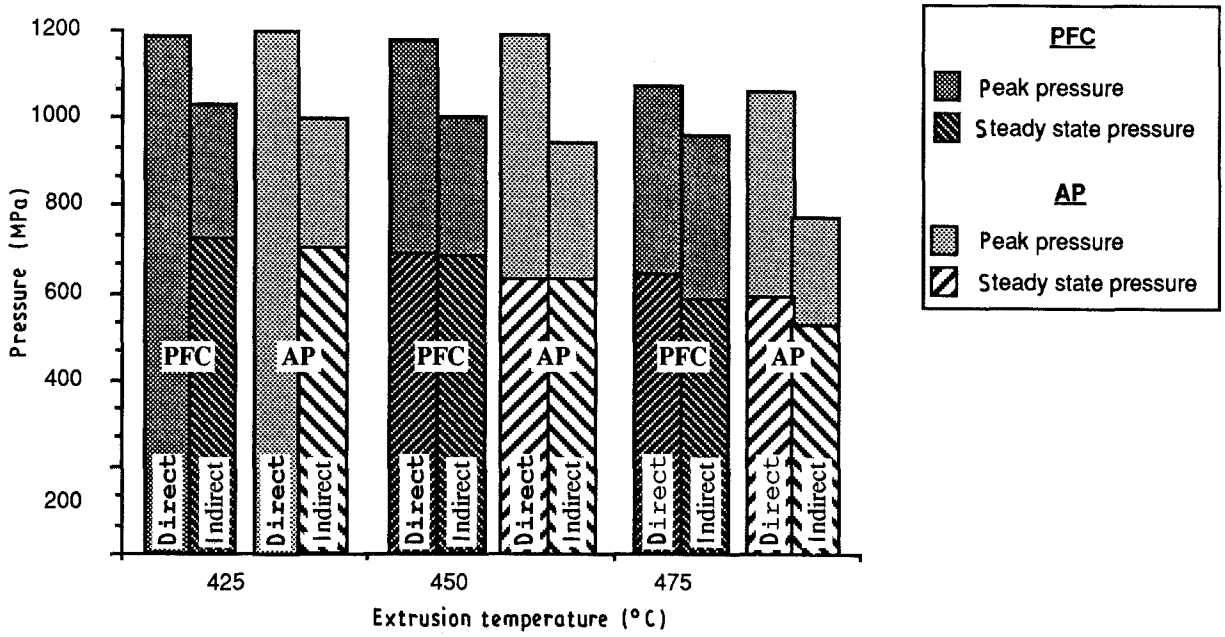

Figure 6 Extrusion pressure requirements as a function of temperature and extrusion mode for both PFC and powder.

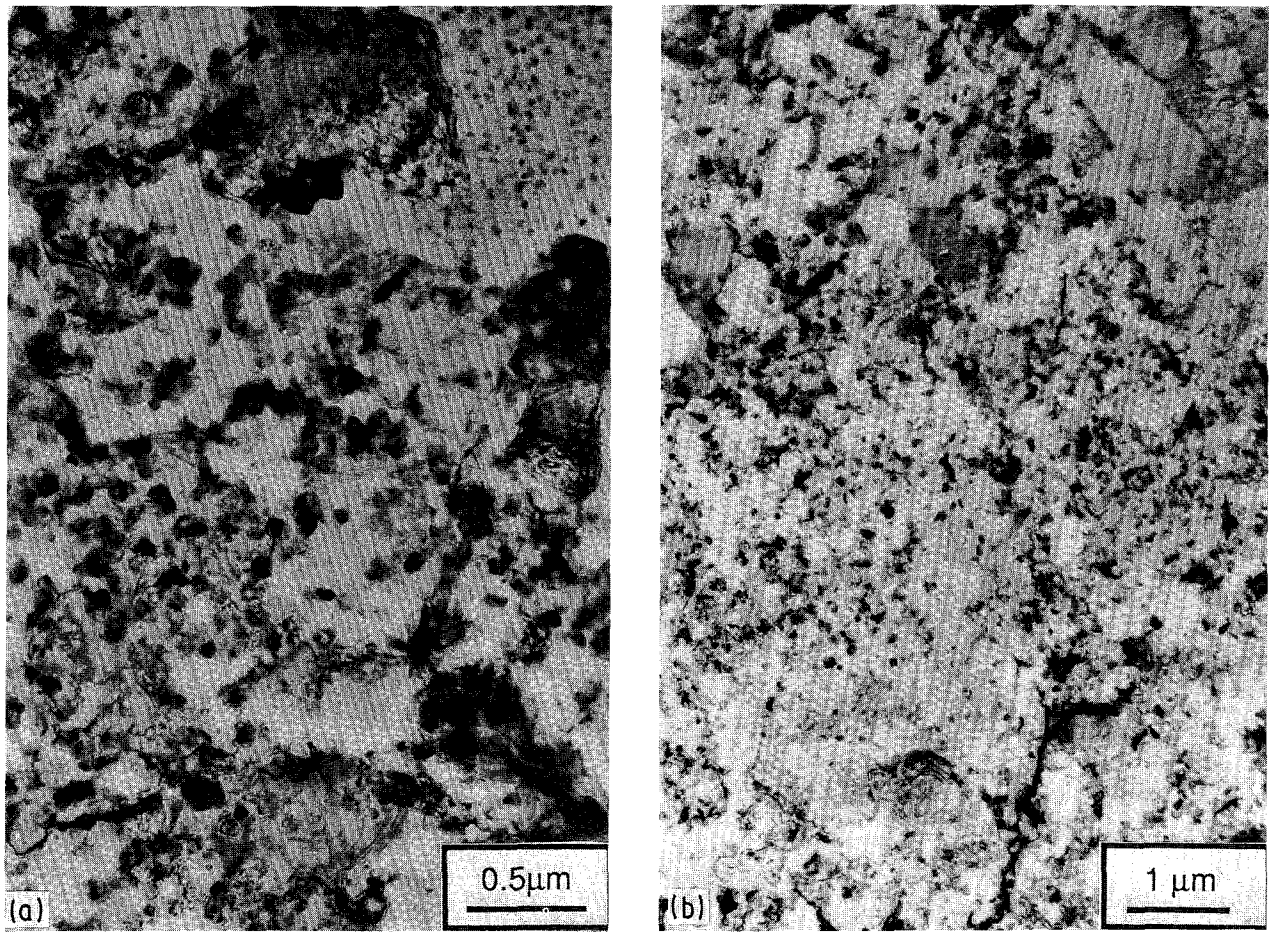

Figure 7 Structure of hot-pressed powders from a partially extruded billet (see text for details).

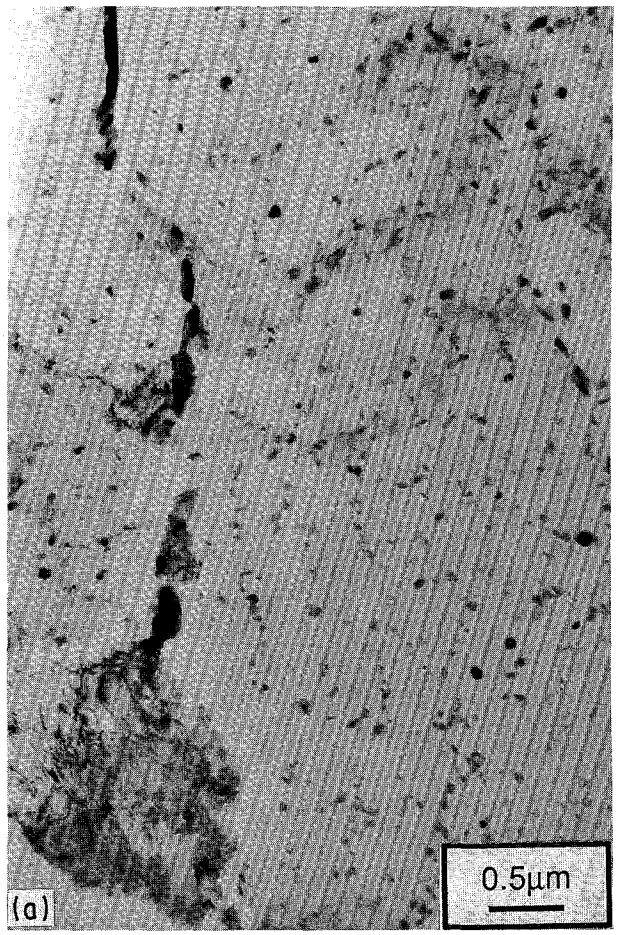

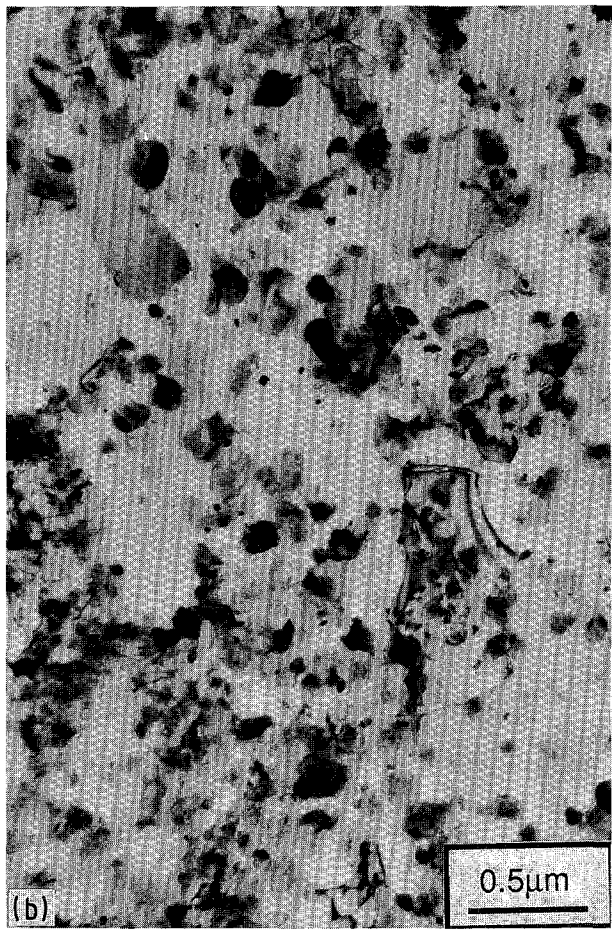

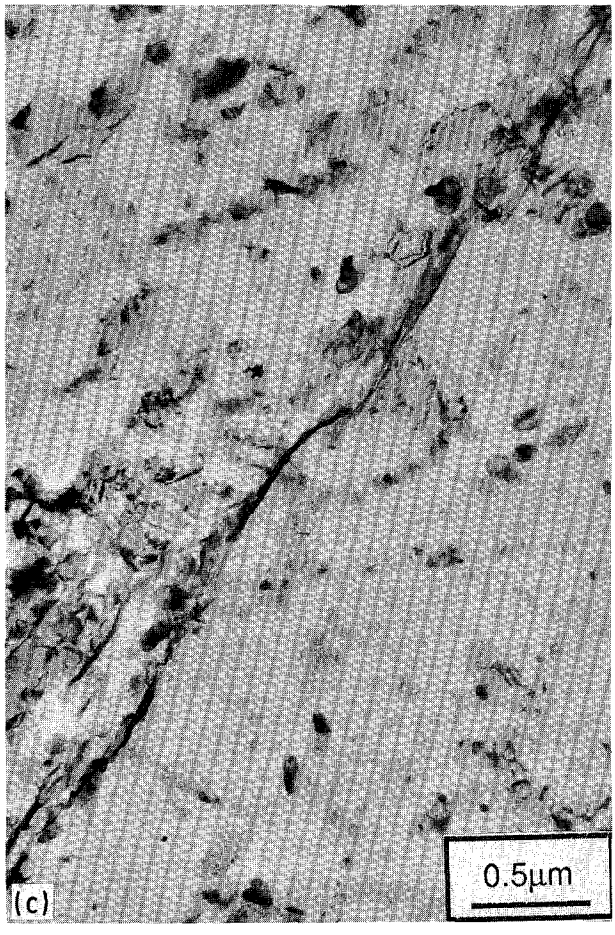

Figure 8 Structure of hot-pressed PFC ribbon from a partially extruded billet: (a) typical cellular structure; (b) effect of coarse dispersoids and (c) oxide break-up.

microstructural heterogeneity of the powder was preserved during processing. The compacted and hot-pressed powders in the partially extruded billet also exhibited a heterogeneous microstructure, Fig. 7a. The original cellular structure (namely, mid-size powders) contains fine scale precipitation of both $Al_{13}Cr_2$ and Al_3Zr whilst the small dispersoids originating from finer powders were unchanged and had stabilized the dislocation substructure, see Fig. 7b, to form small grains and subgrains. In contrast, the more homogeneous PFC ribbon with its typically cellular structure showed evidence of precipitate coarsening during billet preheating, Fig. 8a, and the formation of new precipitates. The precipitate distribution in these regions suggested that the deformation introduced by ribbon chopping had not significantly influenced the decomposition behaviour (compare Fig. 8a with Fig. 4). The other regions originally containing a high number of Cr-rich dispersoids had produced a stabilized dislocation substructure, Fig. 8b, very similar to the compacted powder.

A comparison between powder and PFC revealed no discernible difference in the fragmentation of the surface oxides, see Fig. 8c for example. The critical period for oxide break-up and the formation of metal–metal bonds is when material flows into the extrusion shear zone. As frequently observed in aluminium alloys with high dispersoid densities, the oxide particles become indistinguishable from the intermetallics in the extruded product.

Hardness measurements from the partially extruded billets provided an additional means of monitoring

the decomposition behaviour of the two rapidly solidified particulate. Fig. 9 shows the hardness of material in different billet areas that have experienced various process histories. At the rear of the billet, the particulate has experienced heating to 450 °C and a small amount of deformation. In the shear zone and into the extruded bar, the metal has undergone a more complicated strain and temperature path. Somewhat surprisingly, particulate at the rear of the billet in both cases attained the maximum hardness during processing. The PFC ribbon is 15 VPN harder than the powder which explains the need for larger extrusion pressures and is due to more effective precipitation from the as-solidified supersaturated matrix. In both PFC and powder the alloy softens with passage through the shear zone, die throat and into the extruded bar with a loss of ~50 VPN from the maximum hardness at the rear of the billet. This clearly demonstrates the influence of strain assisted diffusion on precipitation and coarsening kinetics. It also provides a warning against applying the results of static annealing treatments to dynamic situations like hot extrusion.

In terms of the Al–Cr–Zr alloys, the overageing of the microstructure which caused the loss in hardness during processing, confirms the need to reduce the consolidation temperature. This will improve both the final extrusion properties and also reduce the age hardening prior to extrusion, thereby using the RS particulate in its softer condition for ease of consolidation. This latter point is one of the benefits of Al–Cr–Zr system in comparison with the Al–Fe based high temperature alloys which are fully hard after solidification.

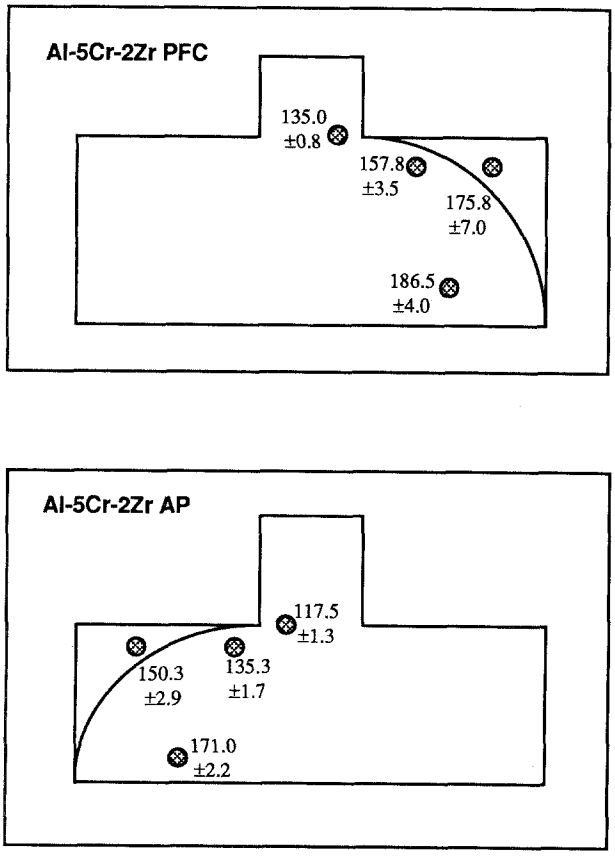

Figure 9 Hardness plots through sections of PFC and powder billets.

3.3. Extrudate structure and properties

The extrudate microstructure has been examined as a function of rapid solidification process and consolidation route. The extruded powder was generally more heterogeneous than the PFC because of the microstructural variability within the atomized powder batch. Fig. 10a shows an example of this hetero-

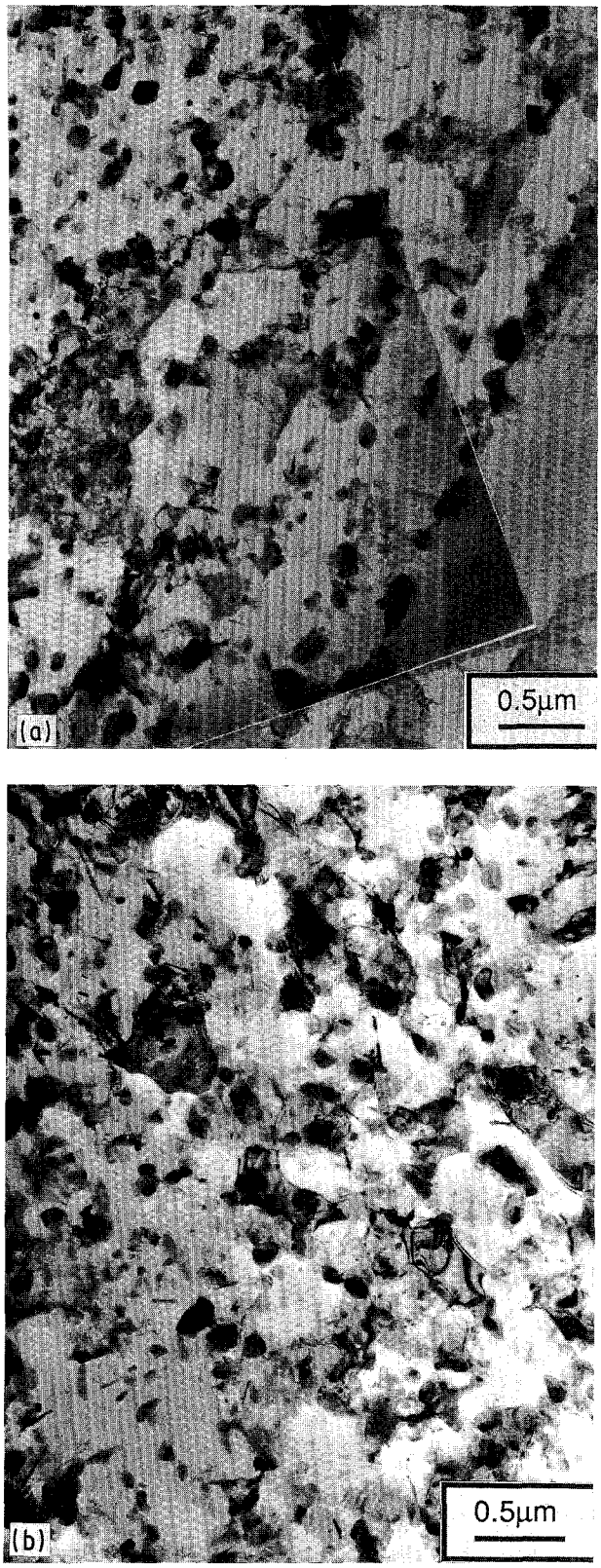

Figure 10 Powder extruded at 450 °C: (a) direct and (b) indirect.

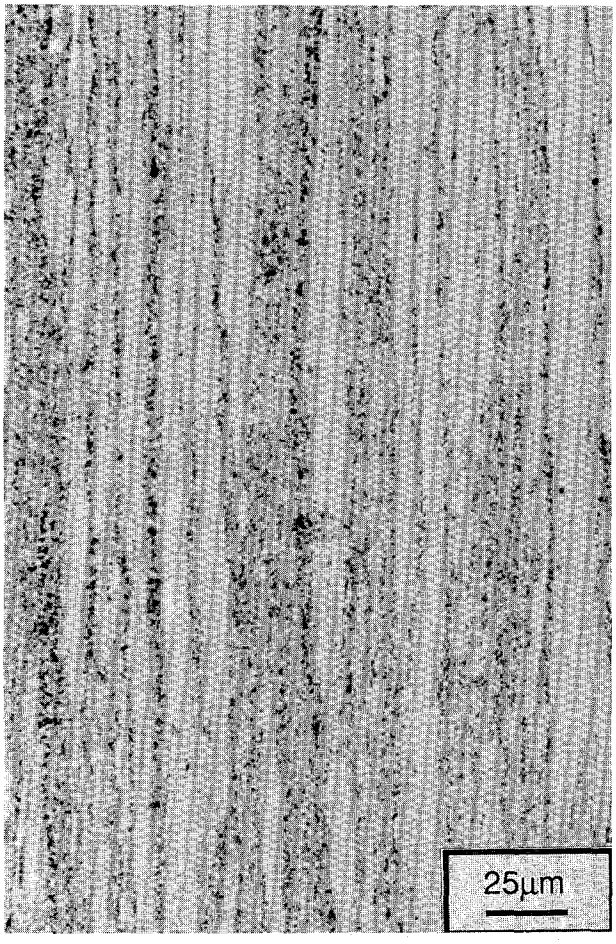

Figure 11 Optical micrograph showing the banded nature of the PFC extrusion.

geneity, in particular the non-uniform distribution of dispersoids and the resultant variable subgrain size. A comparison of powder extruded by direct and indirect modes showed no difference in microstructural heterogeneity. Fig. 10b is a representative micrograph of powder indirectly extruded. The main structural features of the extruded powder were the fine subgrain size (0.2–1.0 μm), stabilized by an array of 0.2–0.5 μm diameter dispersoids and a random distribution of finer precipitates. Powder particle boundaries and oxide stringers, reported in other aluminium alloy powders [11], were not observed in the Al–Cr–Zr extrusions.

In comparison with the consolidated powder, the extruded PFC ribbon exhibited a more homogeneous microstructure which, nevertheless, was extremely fibrous. The fibrous microstructure resulted from a combination of the extrusion process and the anisotropic cellular morphology of the original PFC ribbon (see earlier). This can be seen quite clearly in Fig. 11. In particular, the precipitates had formed and grown at the original cell boundaries during billet preheating and the directionality of the cells had been preserved during deformation. Fig. 12 shows that the fibrous microstructure was present irrespective of the extrusion temperature or the mode of extrusion. Although the majority of the extrudate contained an elongated substructure which was controlled by the fine precipitates, there were also regions with an equiaxed subgrain morphology. The equiaxed structure was created by coarser dispersoids than those

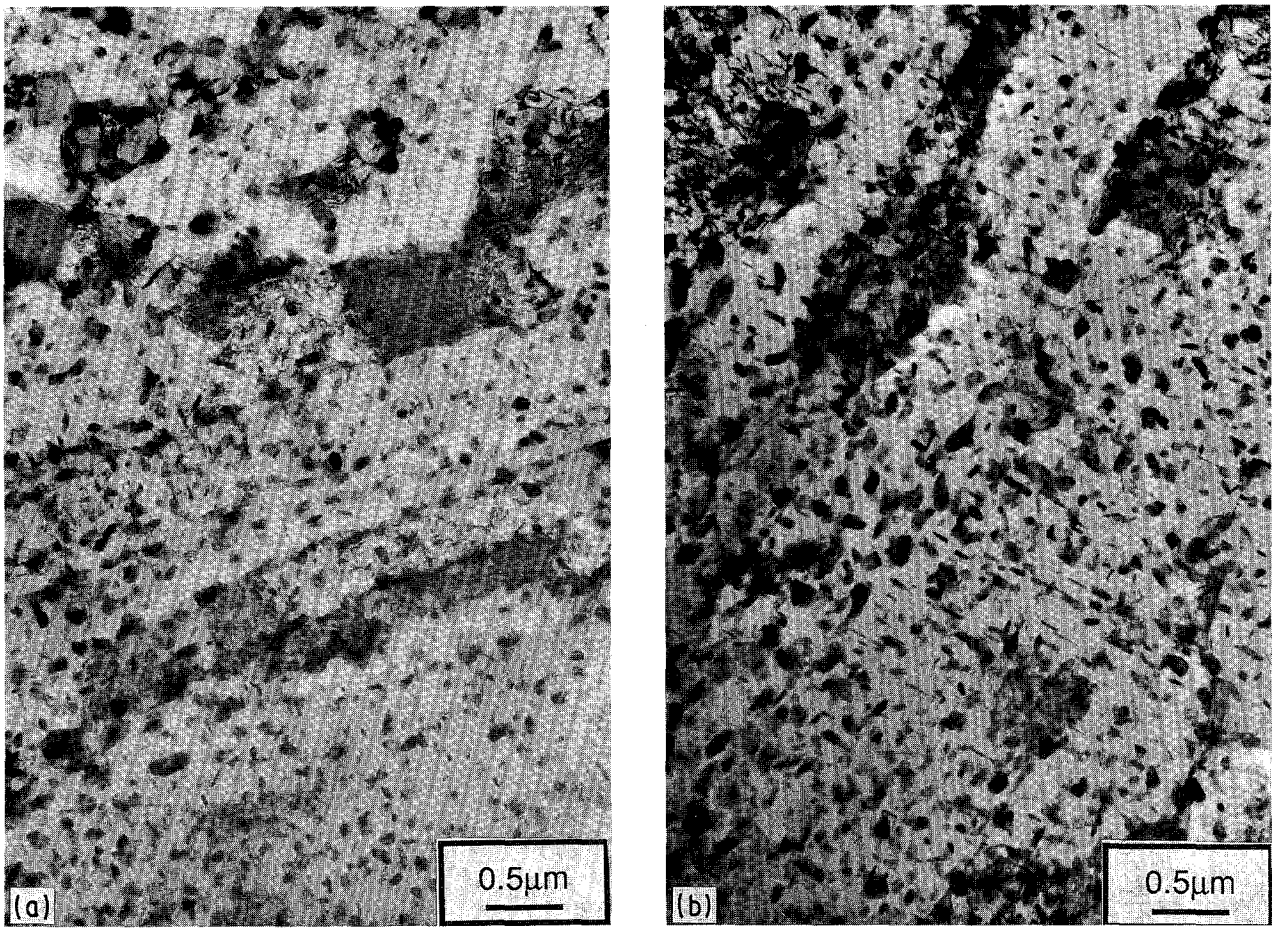

Figure 12 PFC extruded microstructures: (a) 450 °C, direct and (b) 450 °C, indirect.

shown in Fig. 12 and had originated from the high volume fraction of Cr-rich dispersoids observed in the as-solidified ribbon (see Fig. 5b).

In the present study, room temperature tensile tests and short-rod fracture toughness have been used to compare the two RS particulate sources and to evaluate the influence of extrusion route. For a comparison of the tensile data with aerospace target properties for high temperature aluminium alloys, the reader is referred to other recent articles [4, 5].

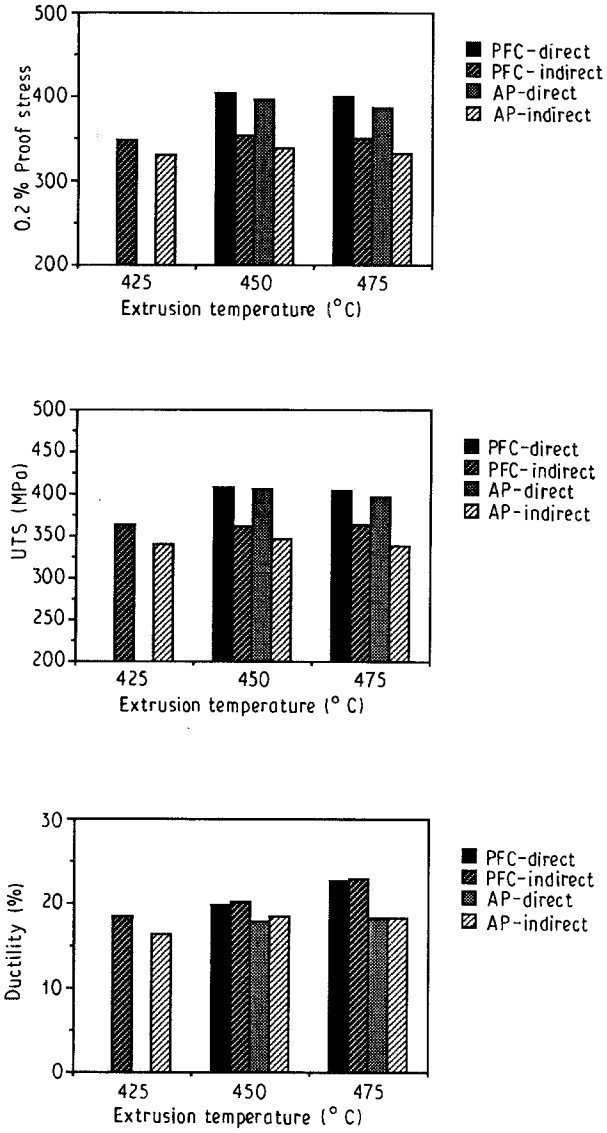

Figure 13 Mechanical properties of round bar extrusions.

The tensile test data for round bar extrusions, Fig. 13, shows that the extrusion mode had the most pronounced influence on strength. A significant strength improvement, both proof and ultimate, was shown by directly extruded metal when compared with indirect, this equally applies to both atomized powder and PFC ribbon. However, it was not possible to observe a microstructural difference between directly or indirectly extruded metal. The features known to influence the strength of dispersion hardened powder alloys are subgrain size, dislocation density and dispersoid size and volume fraction. Unfortunately, the heterogeneous powder microstructure did not allow a quantitative assessment of these features. Conversely, the PFC extrudates which were microstructurally more homogeneous and therefore easier to interpret did not show significant changes to explain the strength improvement.

Extrudates from PFC ribbon had higher strengths than the powder for a given process history and also showed consistently higher strains to failure. However, it must be noted that the tensile ductilities of all Al–Cr–Zr variants were excellent which is in agreement with previous work [1–3] and an important advantage of this alloy system. The property improvement of the PFC is due to the more uniform microstructure and the lack of coarse dispersoids ($> 0.5\,\mu m$) or particle clusters which allows more fine precipitation. Thus the refined microstructure of the PFC ribbons permits a greater proportion of the Zr concentration to contribute to the strengthening and allows more Cr to remain in solid solution to aid thermal stability. Elimination of the coarse dispersoids in the PFC source will also aid tensile ductility which confirms the benefits reported with powders [3] that had been sieved to $< 38\,\mu m$ to remove the coarse

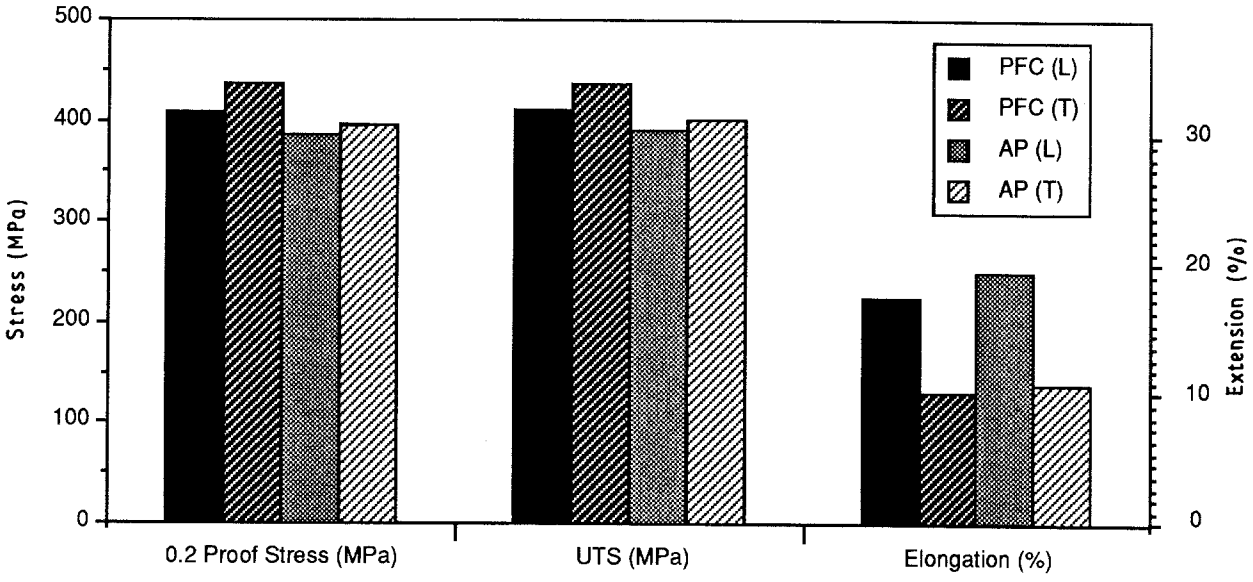

Figure 14 Longitudinal and transverse tensile properties from rectangular bar extrusions.

powders and hence the large dispersoids and precipitate clusters.

The elastic modulus has been measured for the PFC round bar extrusions and a value of 80.5 GPa is in good agreement with the extruded powder, 80.8 GPa, reported elsewhere [3]. This represents a 13% increase over the currently used high temperature aluminium alloy AA2618.

It was anticipated that the fibrous microstructure in RS particulate extrusions would only show the detrimental effects of poor powder/particulate bonding, inadequate degassing or oxide stringers when tested in the transverse direction. To evaluate anisotropy in the powder and PFC extrusions, rectangular geometry bars were extruded and longitudinal and transverse tests performed, Fig. 14. In the longitudinal direction the properties are equivalent to those from round bar (Fig. 13) indicating that the two extrusion ratios and geometries have little influence on strength. In comparison the transverse strengths, proof and ultimate, were 25 and 10 MPa higher for extruded PFC and powder, respectively. Correspondingly, the failure strains in the transverse direction were considerably lower than those for longitudinal specimens but the over-all level was extremely good. A comparison of data from other high temperature aluminium alloys [12] shows that tensile elongations are usually well below 10% thus demonstrating a considerable advantage of the Al–Cr–Zr system.

The results of fracture toughness testing on round bar extrusions is shown in Fig. 15. There is no clear influence of either rapid solidification route or extrusion mode, indeed increasing the extrusion temperature produced the most significant improvement in fracture toughness. Equivalent results for powder and PFC showed that in the longitudinal direction at least, the coarse dispersoids in the powder were not detrimental to fracture properties which is in disagreement with earlier findings [3].

Examination of fracture surfaces from extrudate exhibiting high and low toughness values revealed no structural differences. However close inspection indicated that the surfaces contained fine dimples of approximately 0.5–2.0 μm in diameter. The powder extruded at 450 °C (11 MPa $m^{1/2}$) had a wider range of dimple size, Fig. 16a, than similar PFC extrudate (14 MPa $m^{1/2}$), Fig. 16b. The dimple sizes were of the order of the extrudate subgrain sizes which were controlled by the dispersoid distribution. The variable subgrain size in powder extrusions and hence the range of dimple sizes observed, apparently decreased the fracture toughness. However the fracture surfaces from extrudates with the best toughness were similar to Fig. 16 and did not reveal any significant microstructural difference to account for the improvement.

Finally, Fig. 17 shows the elevated temperature tensile properties of the two consolidated particulate, tested after 100 h at 350 °C. To assess extrusion temperature two extruded bars from each material were evaluated. The data indicates that on a strength comparison the PFC and powder are equivalent but the PFC exhibits significantly higher strains to failure. There is also a small increase in strength after extruding at the higher temperature.

4. Conclusions

A comparative study of inert gas atomized and planar flow cast Al–Cr–Zr alloy consolidated by direct and indirect extrusion has enabled the following conclusions to be made:

1. Planar flow casting produces a more homogeneous microstructure which substantially eliminates coarse dispersoids (> 0.5 μm) and reduces precipitation in the as-solidified ribbon. Thus more solute is retained in supersaturated solid solution when compared with the atomized powder.
2. Both PFC ribbon and atomized powder harden by precipitation of Al_3Zr during preheating of cold compacted billets prior to extrusion. The PFC hardens more due to the uniform ribbon structure and therefore required greater extrusion pressure than the powder.
3. The reduced friction during indirect extrusion significantly reduced the peak pressure needed for both powder and PFC consolidation. Hence it was possible to lower the extrusion temperature by 25 °C.
4. A study of partially extruded billets indicated that

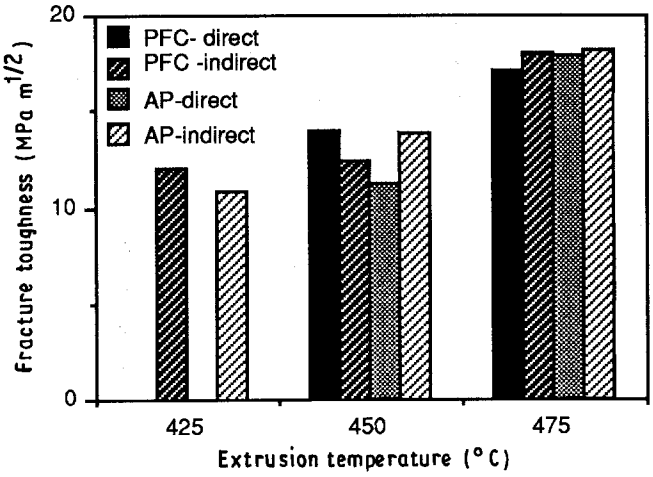

Figure 15 Fracture toughness of round bar extrusions.

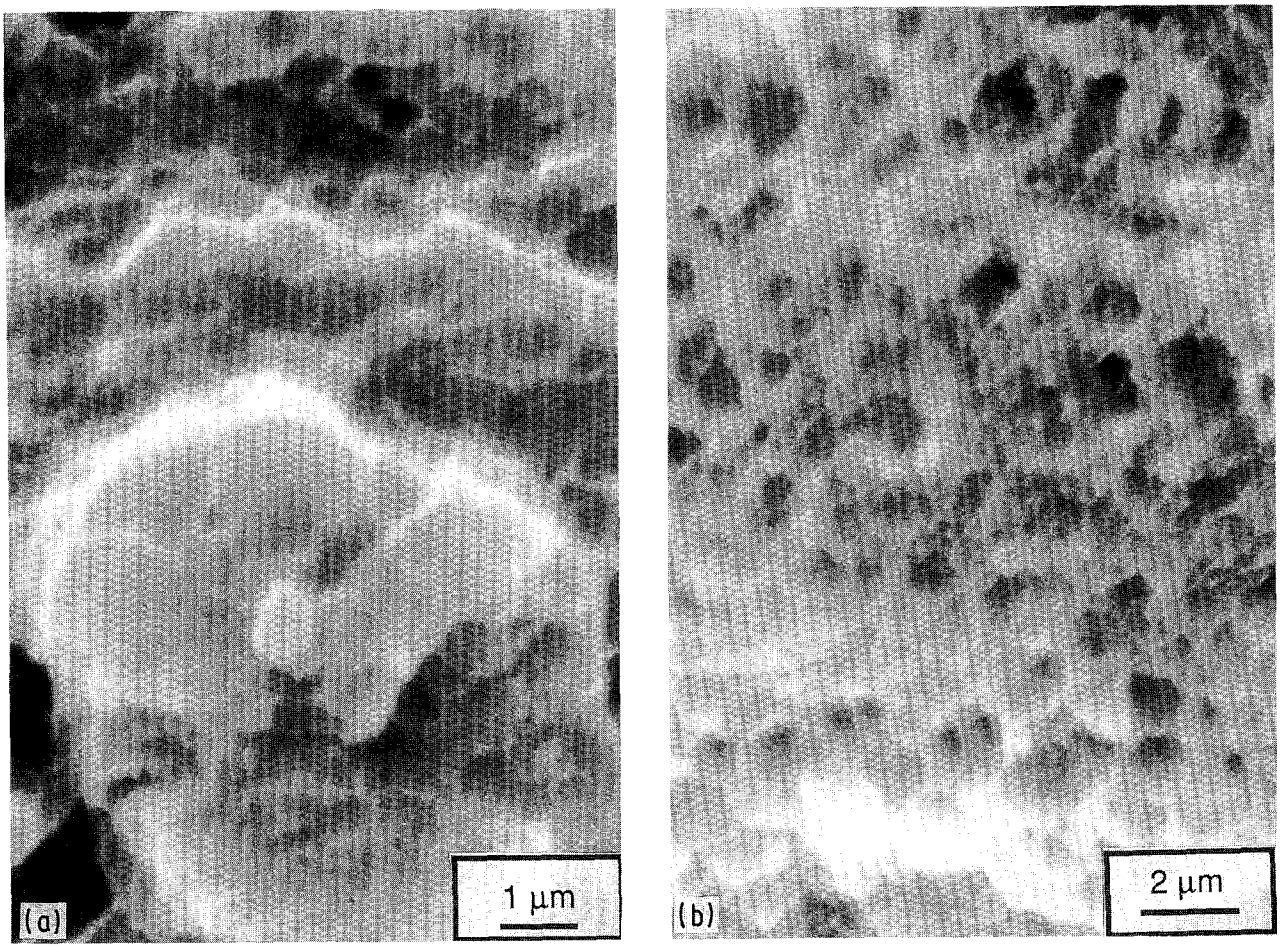

Figure 16 Fracture surfaces from short rod test pieces; (a) powder and (b) PFC.

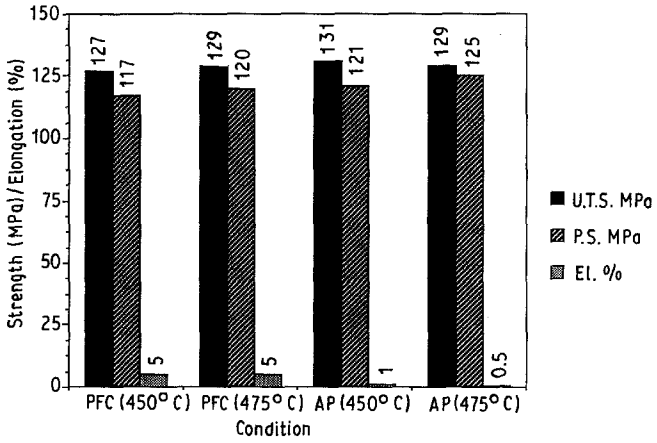

Figure 17 Elevated temperature tensile properties of powder and PFC extrusions.

overageing of both PFC and powder microstructures occurred during the extrusion cycle at 450 °C. This demonstrated the effect of strain assisted diffusion in promoting the precipitation and coarsening of the $Al_{13}Cr_2$ and Al_3Zr phases.

5. The strongest products were produced from direct extrusion of the PFC ribbon when tested in both longitudinal and transverse orientations. All metals tested exhibited a strain to failure greater than 10% and thus demonstrated a major advantage of the Al–Cr–Zr alloys. Elevated temperature tests showed little difference between the two particulate sources except an improvement in ductility from the PFC.

6. Short rod fracture toughness data showed a range from 11–18 MPa $m^{1/2}$ for the extrusions tested. While there was no difference in the behaviour of PFC and powder, the extrusion temperature was found to have the most pronounced influence but without significantly affecting strength.

References

1. G. J. MARSHALL, I. R. HUGHES and W. S. MILLER, *Mat. Sci. Technol.*, **2** (1986) 394.
2. W. S. MILLER and I. G. PALMER, *Metal Powder Report*, **41** (1986) 761.

3. I. G. PALMER, M. P. THOMAS and G. J. MARSHALL, in "Dispersion strengthened aluminium alloys", edited by Y.-W. Kim and W. M. Griffiths (TMS, 1988) p. 217.
4. I. F. SAKATA and S. L. LANGENBECK, *Aerospace Eng.* **April** (1984) 5.
5. W. E. QUIST and R. E. LEWIS, in "Rapidly solidified powder aluminium alloys", edited by M. E. Fine and E. A. Starke Jr. (ASTM STP 890, 1986) p. 7.
6. D. J. SKINNER, K. OKAZAKI and C. M. ADAM, *ibid*, p. 211.
7. J. H. UNDERWOOD, S. W. FREEMAN and F. I. BARATTA (eds): "Chevron notched specimens: testing and stress analysis" (ASTM STP 855, 1984).
8. W. S. MILLER, I. R. HUGHES, I. G. PALMER, M. P. THOMAS, T. SAINI and J. WHITE, in "High strength powder metallurgy aluminium alloys II", edited by G. J. Hildeman and M. J. Koczak (AIME, 1986) p. 311.
9. E. K. IOANNIDIS and T. SHEPPARD, *Mat. Sci. Technol.*, **6** (1990) 536.
10. H. OCTOR and S. NAKA, *Phil. Mag. Letters*, **59** (1989) 229.
11. Y.-W. KIM, W. M. GRIFFITH and F. H. FROES, *J. Metals*, **37** (1985) 27.
12. T. E. TIETZ and I. G. PALMER, in "Advances in powder technology", edited by G. Y. Chin (ASM, Louisville, 1981) p. 189.

Received 26 February
and accepted 1 July 1991